Surfaces and Interfaces 27 (2021) 101486

Contents lists available at ScienceDirect

Surfaces and Interfaces

journal homepage: www.sciencedirect.com/journal/surfaces-and-interfaces

Surface-active extracts from plants rich in saponins – effect on lipid mono- and bilayers

Kamil Wojciechowski [a,b,*], Ilona Jurek [a], Ilona Góral [a,b], Mario Campana [c], Thomas Geue [d], Thomas Gutberlet [e]

[a] Faculty of Chemistry, Warsaw University of Technology, Noakowskiego 3, Warsaw 00-664, Poland
[b] SaponLabs Ltd., Noakowskiego 3, Warsaw 00-664, Poland
[c] Science & Technology Facilities Council, Rutherford Appleton Laboratory Harwell, Oxford, Didcot, United Kingdom
[d] Laboratory for Neutron Scattering and Imaging, Paul Scherrer Institute, Forschungsstrasse 111, PSI, Villigen 5232, Switzerland
[e] Forschungszentrum Jülich GmbH, Jülich Centre for Neutron Science, Jülich 52425, Germany

ARTICLE INFO

Keywords:
Surface tension
Foaming
Supported bilayer
Neutron reflectivity
DLS

ABSTRACT

The aqueous extracts of the seeds of oat (*Avena sativa* L.), horse chestnut (*Aesculus hippocastanum* L.), soybean (*Glycine* max L.), cowherb (*Vaccaria hispanica* [P. Mill.] Rauschert) and quinoa (*Chenopodium quinoa* Willd.), and the roots of soapwort (*Saponaria officinalis* L.) without any preservatives were characterized in terms of their surface tension, surface compression (dilational) rheology, foamability and foam stability. The saponin content in the extracts was determined using UPLC-MS and their interaction with model lipid monolayers consisting of dipalmitoylphosphatidylcholine (DPPC)/cholesterol and Ceramide AP/stearic acid/cholesterol were analyzed by surface pressure relaxation, surface compression elasticity and neutron reflectometry (NR). The lipid composition was chosen to mimic the cell membrane of keratinocytes – major constituents of the human deeper skin layers, and the intercellular lipids ("mortar") in the "bricks and mortar" model of the outermost layer of the epidermis (*stratum corneum*). Bilayers of DPPC/cholesterol were additionally characterized using dynamic light scattering (DLS) and NR. The oat and soybean extracts were shown to be much less abundant in saponins as compared to cowherb, horse chestnut, soapwort or quinoa, and showed limited foaming abilities. They did not affect significantly the model lipid mono- and bilayers mimicking the skin outer layers, either. The horse chestnut extract affected both model membranes to the highest extent, yet without solubilizing the lipids.

1. Introduction

Plant extracts have always played a very important role in human life, providing a number of nutritional, medicinal, detergent or cosmetic ingredients. Only the last few decades of extensive exploration of non-renewable resources allowed humankind to develop the low-cost and efficient synthetic replacements for the natural compounds, especially in medicine and detergent/cosmetic applications. Nevertheless, in many aspects the plant-derived chemicals are still superior to their synthetic analogues. Biosurfactants belonging to the group of saponins are especially good examples of such superiority in view of their unique ability to rigidify the interfacial layers [1–3]. In this respect they even outperform several surface-active proteins, known to form highly viscoelastic adsorbed layers providing exceptional stability to foams and emulsions [4–6]. An additional advantage of saponins over the high-molecular weight proteins are their smaller molecular dimensions and consequent higher diffusion coefficients. Although saponins are a very diverse group of molecules, their common structural feature is the presence of two fragments of different polarity: triterpenoid or steroid aglycon (non-polar part) and typically 1–3 oligosugar glycons (polar part). Saponins are synthesized by numerous organisms, mostly plants [7]. Their widespread presence renders them important components of our daily diet (soybeans, chickpeas, peanuts, beans, lentils, peas, spinach, oats, asparagus, fenugreek, garlic, sugar beets, potatoes, green peppers, tomatoes, onions or tea, to name just a few) [8].

While the saponin intake with food has not changed drastically over the last centuries, the increasing popularity of natural cosmetics raises some questions concerning the effect of saponins on human skin. In this context it is important to mention a strong affinity of many saponins to lipids and especially to sterols present in biological membranes of many

* Corresponding author at: Faculty of Chemistry, Warsaw University of Technology, Noakowskiego 3, Warsaw 00-664, Poland.
E-mail address: kamil.wojciechowski@ch.pw.edu.pl (K. Wojciechowski).

https://doi.org/10.1016/j.surfin.2021.101486
Received 11 May 2021; Received in revised form 10 September 2021; Accepted 17 September 2021
Available online 29 September 2021

living organisms (e.g. cholesterol in mammals or ergosterol in fungi) [9–13]. Saponin-rich plants probably employ this strong affinity to defend against pathogens (bacteria, fungi, insects, herbivores) [14–16]. Several recent studies suggest that many saponins do not solubilize the lipid layers constituting biological membranes but rather fluidize them, effectively enhancing their permeability [3,12,17–19]. This unique feature of saponins clearly differentiates them from the usually much more aggressive synthetic surfactants which often solubilize lipid monolayers under similar surface pressure values. In other words, some saponins and saponin-rich extracts can offer more rigid adsorbed layers and lower membranolytic activity than their simple synthetic counterparts (e.g. sodium dodecyl sulfate, cetyltrimethylammonium bromide, Triton X-100), while providing comparable ability to reduce surface tension [3,17].

Drying strongly foaming aqueous solutions is a challenging task, especially when using methods based on bulk solvent evaporation. To avoid problems with extensive foaming, alternative techniques can be used, e.g. spray-drying. However, the process efficiency is often low, and drying aids are usually required to improve it. In our previous contributions we successfully spray-dried several plant extracts using a mixture of sodium benzoate and potassium sorbate as preservative and drying aid [20–22]. However, the quantitative composition of such spray-dried powders is not necessarily the same as that of the extract. Consequently, any surface activity studies of such extracts are flawed by the unknown exact content of the extracted mass.

In this contribution, thanks to a careful optimization of the extraction and spray-drying protocols, the dried extracts without any additives were achieved. They were characterized qualitatively by UPLC-MS and their surface properties were assessed by employing surface tension/compression rheology and foaming properties. Their effect on lipid monolayers mimicking the human skin layers (lipid membranes of keratinocytes and intercellular lipid mixture) was analyzed using surface pressure relaxation and compression rheology in Langmuir trough, supported by neutron reflectivity at air/water interface. Analogous experiments were performed with the corresponding lipid bilayers using dynamic light scattering and neutron reflectivity at Si/water interface.

2. Material and methods

Milli-Q water (Millipore, France) was used to prepare all solutions. Its surface purity was confirmed by monitoring dynamic surface tension for 1 h. Similar tests were run for all glassware, by measuring surface tension of the last water portion used for rinsing the glassware. All glassware was cleaned with Hellmanex II solution (Hellma, Worldwide) and acetone prior to rinsing with Milli-Q water. For the NR experiments, D_2O (Sigma Aldrich or Armar Chemicals, Switzerland, 99.8 atom% D) was used, either alone or mixed with the Milli-Q water. The protonated lipids 1,2-dipalmitoyl-sn-glycero-3-phosphocholine (DPPC, Cat. No. P0736) and cholesterol (Cat. No. 26,732) were purchased from Sigma-Aldrich, Poland. The deuterated lipids (1,2-dipalmitoyl-d_{62}-sn-glycero-3-phosphocholine - DPPC-d_{62} and cholesterol-d_7) were purchased from Avanti Lipids, USA. Sodium laureth sulfate (ethoxylated sodium dodecylsulfate, SLES) was kindly provided by PCC Exol (Brzeg Dolny, Poland). The details of the herbal material used in the study are collected in Table 1.Soybean seeds were purchased from BRAT.pl sp. z o.o., Poland, oat seeds from Niro, Poland (mixture of hulless varieties from ecological agriculture), quinoa seed hulls from Irupana Andean Organic Food S.A. (a mixture of varieties cultivated in Bolivia), cow herb seeds from Canadian Carnation BioProducts Company LLC, Canada, horse chestnuts from Astex Ltd, Poland (collected from the wild state) and soapwort roots from Dary Natury (Koryciny, Poland). The voucher specimens were deposited in Herbarium of the University of Warsaw (Poland).

All extracts were obtained and stored as dry powders as described in ref. [22] but without any preservatives/drying aid. Briefly, maceration was performed at room temperature for 24 h, infusion (pouring water at 95 °C and left for cooling) - during 30 min, and decoction (boiling) - during 2 h. For optimization of the extraction method, the extracts were separated by centrifugation (3000 rpm, 15 min) and filtering through a 5 μm syringe filters. The choice of the optimum extraction conditions was made on the basis of the dry mass extracted, determined using a moisture analyzer (ATS60, Axis, Poland). For the remaining experiments, a Colombo 18 OIL filter press (Rover Pompe, Italy) using paper plates with pore sizes of 15 μm, 11 μm, 6 μm and 3 μm was employed. The filtered extracts were dried using a YC-015A lab spray dryer (Pilotech, China). The chamber temperature was set to 120 °C and the outlet temperature (effective drying temperature) equaled typically ~70 °C. The drying conditions were optimized with help of a design of experiment (DOE) method using a Design Expert 11 software (Stat-Ease, Inc., USA).

UPLC-MS analyses were performed at the Institute of Soil Science and Plant Cultivation in Pulawy (Poland) using a Waters ACQUITY UPLC system (Milford, MA, USA) equipped with a binary solvent manager and coupled to a Waters ACQUITY TQD (tandem quadruple mass detector) with an electrospray ionization (ESI) source (for cowherb and soapwort extracts) or an ACQUITY I-Class UPLC system equipped with a XEVO TQS-micro triple quadrupole mass spectrometry (Waters Corp., Milford, MA, USA) (for oat, soybean, horse chestnut and quinoa extracts). The details were described in our previous paper [22]. The following purified saponins were used for calibration: escin (Sigma-Aldrich) (for horse chestnut), soyasaponin I (for soybean and quinoa, own isolation), avenacoside A and B (for oat, own isolation) and saponarioside I (for

Table 1
The details of the employed plant material together with the optimized extraction and spray-drying conditions as well as the HPLC-determined saponin content for the extracts obtained without any additives.

Common name	soybean	oat	quinoa	cow herb	horse chestnut	soapwort
Latin name	*Glycine* max *(L.) Merr.*	*Avena sativa* L.	*Chenopodium quinoa* Willd.	*Vaccaria hispanica* [P. Mill.] Rauschert	*Aesculus hippocastanum* L.	*Saponaria officinalis* L.
Plant organ	seeds	seeds	seed hulls	seeds	seeds	root
Voucher specimen number	WA00000 98,196	WA00000 98,194	WA00000 98,195	WA00000 98,198	WA00000 98,193	WA00000 98,197
Extraction method	macerate	macerate	macerate	decoction	macerate	decoction
plant material-to-water ratio [g/g]	0.15	0.25	0.05	0.05	0.10	0.05
Extraction time [min]	180	240	120	15	180	15
Extraction yield [%]	10.4	2.1	12.3	3.1	16.7	44.8
Spray-drying temperature [°C]	126	123	130	165	160	187
Spray-drying air flow [l/min]	193	187	212	205	212	170
Spray-drying feed rate [ml/min]	12.3	6.5	17.3	18.9	15.6	22.3
Drying yield [%]	61.1	52.4	63.3	42.3	66.6	52.9
Total saponin content in the dried powder [%]	0.03 ± 0.00	< 0.01	20.73 ± 0.61	1.72 ± 0.08	11.42 ± 0.31	73.90 ± 2.08

soapwort and cowherb, own isolation).

The dried extracts were stored at room temperature and were dissolved prior to the analysis in Milli-Q water to achieve the required concentration and then filtered through a 0.45 μm syringe filter. To prevent microbial decomposition of the extract components, a commercial preservative Euxyl K500 (Schülke & Mayr GmbH, Germany, containing ~20% diazolidinyl urea, ~20% sodium benzoate and ~10% potassium sorbate) was added to the soybean, oat, and cowherb reconstituted extracts at 0.15%. For horse chestnuts, soapwort and quinoa, a mixture of sodium benzoate (0.0625%) and potassium sorbate (0.075%) was employed.

The surface tension and surface dilatational rheology measurements were performed using a drop profile analysis tensiometer PAT-1 (Sinterface Technologies, Germany), as described previously [21].

Foamability of each extract was tested according to Bikerman method using a home-built setup consisting of three glass columns (40 cm high, 20 mm diameter) with glass frits (G4) connected to a compressed N_2 bottle through a 3-way valve as described in [23]. After filling the three columns with 5 ml of the reconstituted extract, the nitrogen gas (99.9%) was purged through the frits for 30 s at a 3 L/h flow to produce the foam. The foam height in all three columns was used to calculate the average and standard deviation for a given extract at $t = 0$, 2, 3, 5 and 10 min to determine the foam height, $h(t)$.

The Langmuir monolayer experiments were performed using two mixed lipid mixtures. The first contained Ceramide VI (CER), stearic acid (SA) and cholesterol (CHOL) in a molar ratio of 1:1:0.7 (CER/SA/CHOL) and the second - 1,2-dipalmitoyl-sn-glycero-3-phosphocholine (DPPC) and cholesterol (CHOL) in a molar ratio of 7:3 (DPPC/CHOL). The surface pressure relaxation curves after a quick compression to Π_0= 30 mN/m, $\Pi(t)$, for the monolayers on pure water and on the 1% plant extract solution were recorded using a home-built Langmuir trough equipped with a Wilhelmy plate made of filter paper (ashless Whatman Chr1) connected to an electrobalance (KSV, Finland). The subphase temperature of 21 ºC was controlled by means of a thermostat. The experimental details are given in [24]. The surface pressure was monitored for 6000 s during the subphase exchange procedure. The experiments with the respective Gibbs layers (without the lipid monolayer) were performed analogously, omitting the monolayer deposition and compression steps. At the end of each monolayer relaxation measurement, the surface compression (dilational) response of the monolayer was probed by performing oscillatory movements of the barriers, in analogy to oscillating the drop volume described above for the pending drop experiments. The frequency of 0.1 Hz and the relative amplitude of 2% were used.

The liposomes were prepared using the method of hydration of dry lipid films consisting of DPPC/cholesterol (7:3, mol/mol). A blend of an appropriate lipid composition with a concentration of 2 mg/ml was dried in a stream of compressed air and then hydrated by a phosphate buffer (pH = 7), the sample was mixed and heated in a stream of hot water in order to facilitate detaching of the lipid film from the dish walls. Subsequently the mixture was sonicated (Sonopuls HD 2070, Bandelin, Germany) and extruded (mini-extruder, Avanti Polar Lipids, USA) through a 100 nm filtration membrane (33 times). The liposome dispersions (0.1 mg/ml) were mixed with solutions of dry plant extracts of cowherb, soapwort, horse chestnut, soybean, and oat, prepared directly before measurement in phosphate buffer (pH = 7), with final dry mass content of 0.001, 0.04, 0.2, 1, 5%. The same solutions without liposomes were used as reference.

The particle size distribution was determined by dynamic light scattering (DLS) using a Zetasizer HS3000 (Malvern, UK) immediately after the sample preparation (t_0) and after 120 min of incubation at room temperature (t_1). The phosphate buffer and all solutions of the natural extracts were filtered using 0.22 μm syringe filters. The measurement uncertainty (14%) was determined from six measurements of four independent samples.

A typical neutron reflectivity measurement consists of determining the intensity of a neutron beam, R, reflected from a test surface, normalized to the incoming intensity at a certain angle of incidence, θ. The beam intensity, R, is measured as a function of a scattering wave vector, q, expressed as the incidence angle θ normalized to the corresponding wavelength, λ, as $q = 4\pi \sin(\theta)/\lambda$. The neutron reflectivity (NR) experiments with monolayers at air/water interface were performed at Paul Scherrer Institute (Villigen, Switzerland) using the time-of-flight AMOR reflectometer [25]. The analogous experiments with bilayers at Si/water interface were performed at the time-of-flight reflectometer SURF at the pulsed neutron source at the ISIS Facility, Rutherford Appleton Laboratory (Oxfordshire, U.K.). The NR experiments at air/-water interface were performed for three angles of incidence ($\theta = 0.25°$, 0.65° and 1.4°) using a wavelength range from $3 < \lambda/Å < 12$, covering the necessary q range for the experiments of $q_{min} = 0.01\ Å^{-1}$ to $q_{max} = 0.15\ Å^{-1}$. The resolution was set by a slit system on the incident side and the time-of-flight parameters to $\Delta q = 0.006\ Å^{-1}$. A beam of rectangular cross Section 1 × 35 mm^2 (for low angles) impinged on the sample at the air/water Langmuir trough. The scattered neutrons were recorded with a ^{3}He-single detector tube in time-of-flight mode requiring typically 8 h of beamtime. The average statistical error of the recorded reflectivity varies between 1 and 3% for the lowest and highest angle of incidence applied. The NR profiles of Gibbs layers of the extracts containing 1% of dry weight were recorded at equilibrium (verified using the Wilhelmy balance). Two D_2O/H_2O mixtures, one with 89% D atoms and the second - so called null reflecting water (NRW) – with 14% D atoms, were also employed with the scattering length density (SLD) being 5.62 × 10^{-6} $Å^{-2}$ and 0 $Å^{-2}$, respectively. The experiments were performed using a Langmuir-Blodgett trough equipped with a moving barrier and a trough inset for subphase exchange using a Harvard Apparatus PHD Ultra syringe pump.

The NR experiments at Si/water interface were performed using a polychromatic beam of neutrons with wavelengths in the range $0.5 < \lambda/Å < 6.9$, which was reflected from the interface and detected using a single ^{3}He detector. The full q range was covered using three incident angles: $\theta = 0.35°$, 0.65° and 1.5° Pure D_2O ($SLD = 6.35 \bullet 10^{-6}$ $Å^{-2}$), pure H_2O ($SLD = -0.56 \bullet 10^{-6}$ $Å^{-2}$) and a so called Si-matched water, CMSi, containing 38% D_2O and 62% H_2O ($SLD = 2.07 \bullet 10^{-6}$ $Å^{-2}$) were employed as solvents for the reconstituted extracts. The sample cell was maintained at 25 °C by means of a circulating waterbath and consisted of a PEEK trough covered with the Si substrate, where the solution is exchanged by means of a Hitachi L-7100 HPLC pump. The lipid bilayers were deposited on the Si surface by the vesicle fusion method from 2 mg/ml liposome (DPPC-d_{62}/CHOL-d_7, 7/3 mol/mol) dispersion in phosphate buffer (pH 7, ionic strength, $I = 0.02$ M). The liposomes were prepared by sonication at temperatures above the transition temperature (>50 °C). After deposition, the substrate was left to equilibrate for ~ 1 h and rinsed with the appropriate D_2O/H_2O mixture to provide three neutron contrasts (D_2O, H_2O and CMSi). Measurements were started after a waiting time of at least 30 min to establish equilibrium at the silicon/water interface.

3. Theory/calculation

The equilibrium surface tension values (γ_{eq}) were obtained by extrapolation of the dynamic values ($\gamma(t)$) using the long term approximation of the Ward-Tordai equation (for $1/t \rightarrow 0$) [26]:

$$\gamma_{eq} = \gamma - \frac{RT\Gamma^2}{c_0}\sqrt{\frac{\pi}{4Dt}} \quad (1)$$

where γ is the interfacial tension, γ_{eq} - equilibrium interfacial tension, R - gas constant, T - temperature, D - diffusion coefficient, t - time, c_0 – bulk concentration.

The surface rheological response of the pre-equilibrated adsorbed layers was probed by performing sinusoidal perturbations of the drop volume after 3600 s of adsorption, in the frequency range 0.005–0.1 Hz,

with the amplitude of 5%. The $\gamma(t)$ amplitude and the phase shift with respect to the generated oscillations were obtained from the Fourier transformation of the data, and were used to calculate the real (storage modulus, E') and imaginary (loss modulus, E'') parts of the elasticity modulus [27]:

$$E = \frac{d\gamma}{d\ ln\ A/A_0} = E'(f) + iE''(f) \quad (2)$$

where γ is the interfacial tension, f - frequency of oscillations, A and A_0 - the actual and initial interfacial area, respectively.

The experimentally obtained reflectivity curves at the air/water interface were analyzed by using the Parratt32 software and at the Si/water interface using RasCAL. Both algorithms determine the optical reflectivity of neutrons from planar surfaces using a calculation based on Parratt's recursion scheme for stratified media [28]. The reflecting interface is modelled as consisting of layers of specific thickness, scattering length density and roughness, which are the fitting parameters. The model reflectivity profile is calculated and compared to the measured data, then the model is recursively adjusted by a change in the fitting parameters to best fit the data. The *SLD* of all components is listed in Table S1.

4. Results

In the first step, the extraction conditions were optimized individually for each plant according to the scheme depicted in Supporting Materials. The overall optimized extraction and drying conditions are collected in Table 1.

The total saponin content in the spray-dried extracts was determined by UPLC-MS. The results collected in Table 1 show a very wide spread of the total saponin content between different extracts (< 0.01 - 73.9%) with the lowest saponin content found in the oat seeds extract. This extract was also characterized by the lowest amounts of extractable dry matter (2.1%). Much more material could be extracted from soybeans (10.4%), although only 0.03% of this mass could be assigned to saponins. On the other end of the saponin content scale, the extracts of horse chestnut seeds, quinoa hulls and especially soapwort roots were very rich in saponins. Especially the latter contained high amounts of water-soluble components (44.8%), of which as much as 73.9% were saponins. It is worth noting that the saponin contents in the present extracts (Table 1) are systematically higher than those obtained in presence of potassium sorbate and sodium benzoate (0.022±0.001%, undetectable, 14.95 ± 0.22%, 0.241 ± 0.011%, 10.04 ± 0.11% and 5.09 ± 0.24% for soybean, oat, quinoa, cowherb, horse chestnut and soapwort, respectively) [22].

The surface activity assessment of the extracts started with analysis of their surface tension using a drop shape analysis method in the range of $1\bullet10^{-3}$–$3\bullet10^{\circ}$% of dry extract mass (d.m.). The dynamic surface tension, $\gamma(t)$, results are collected in Fig. S1 (Supporting materials) and the extrapolated equilibrium values, γ_{eq}, as a function of dry extract mass (surface tension isotherms) are collected in Fig. 1. The isotherms for all extracts except for the horse chestnut are rather similar. From the practical perspective, the extracts of quinoa, cowherb, soapwort, oat and soybean offer similar effectiveness of surface tension reduction on the dry mass basis, while that of horse chestnut is less effective. However, one should note that these observations apply to the extracts, not the starting plant material. Should the extraction yield be taken into account, the respective isotherms on the dry plant mass basis would be shifted to the right – slightly for soapwort and significantly for oat and cowherb (cf. Table 1). In other words, given its highest extraction yield, the soapwort root is the most efficient plant material for reducing surface tension in this study. Another interesting observation is that the plant extracts with very different saponin content (Table 1) present quite similar surface tension isotherms. Although it is clear that individual saponins present in different plants differ in their molecular weight and

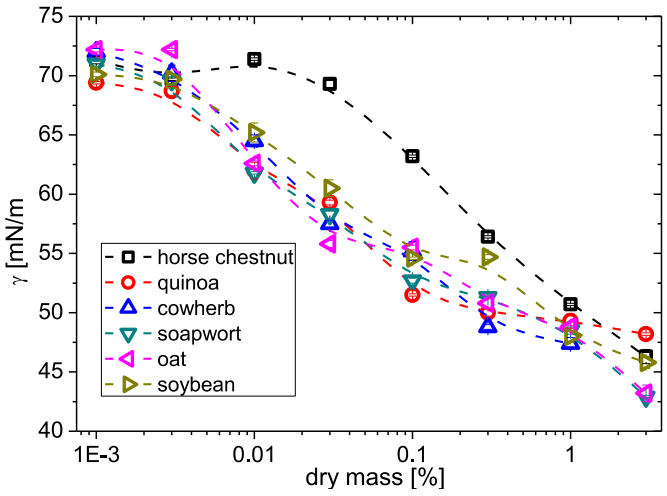

Fig. 1. Surface tension isotherms for the plant extracts.

surface activity, the observed results show that some extracts (especially oat and soybean) probably owe significant part of their surface activity to the non-saponin fractions.

The surface tension isotherms presented in Fig. 1 are useful for describing the ability to lower surface tension and the consequent detergent/foaming activity. However, in the absence of detailed information on chemical composition of the extracts, they cannot be interpreted quantitatively using any adsorption models or even the Gibbs equation. Thus, to obtain more quantitative information on the adsorbed layers, neutron reflectometry (NR) was employed. Practically all hydrogen atoms in the plants (and consequently also in their aqueous extracts) are present in a ^{1}H (protium) form, which results in a relatively low ability to scatter neutrons. In contrast, the ^{2}H (deuterium) form, present e.g. in D_2O, scatters neutrons strongly. We employed this difference between the low-neutron-scattering (air and surface-active components of the extracts) and high-neutron-scattering (D_2O) objects to highlight the presence of the ^{1}H-rich (low-neutron-scattering) adsorbed layers at the D_2O/air interface. For this purpose, we measured neutron reflectivity from the surface of the extracts containing 1% of dry mass dissolved in water containing 89% of its hydrogens in the form of deuterium.

The raw NR curves are shown in Fig. S2. All data was fitted using a 1-layer fit using a constant interlayer roughness of 3 Å, hence the only fitting parameters were the layer thickness, d, and its scattering length density, SLD_{layer}. All reflectivity profiles measured in presence of saponin extracts significantly deviate from that of D_2O, confirming that surface adsorption does occur. The best-fit parameters (SLD_{fitted}, and SLD_{layer}) are collected in Table 2 and represent two possible situations:

(a) the adsorbed layer is fully immersed in water (hence possessing a high volume fraction of D2O and presenting a high SLD value)
(b) the adsorbed layer floats above the water surface (low or null D2O content and hence low SLD value).

Given the hydrophilic nature of the saponins' glycosidic part, at least partial immersion in water seems more likely, although the 1-layer model by definition provides a picture with averaged glycone and aglycone contributions. In reality, probably only the hydrophilic sugar part is genuinely submerged in the aqueous phase, while the aglycone part likely extends toward air, as suggested by surface tension and surface compression rheology results [29,30]. In either case the best-fit values of the layer thickness show that all extracts with high saponin content (horse chestnut, soapwort and cowherb) form rather thin adsorbed layers (20–22 Å), consistent with molecular dimension of saponin molecules. On the other hand, the ones forming in the oat and

Table 2
Best-fit neutron scattering parameters for the adsorbed layers of the plant extracts (1% dry mass) used in this study in the absence (Gibbs layers in D_2O) and presence of DPPC-d_{62}/CHOL-d_7 lipid monolayer on NRW compressed initially to $\Pi_0 = 30$ mN/m. Background reflectivity was set to 10^{-6} Å^{-2}. For the Gibbs layer in D_2O two values for *SLD* are presented (SLD_{fitted}, and SLD_{layer}), see the text.

Gibbs layer in D_2O			
Subphase D_2O (89% D)	layer thickness [Å]	SLD_{fitted} [10^{-6} Å^{-2}]	SLD_{layer} [10^{-6} Å^{-2}]
D_2O	–	5.62±0.03	
soapwort	21.2 ± 1.0	1.09±0.12	4.53 ± 0.12
soybean	45.8 ± 0.5	1.28±0.03	4.34 ± 0.03
oat	27.9 ± 0.5	1.01±0.05	4.61 ± 0.05
cowherb	20.3 ± 1.0	1.09±0.07	4.53 ± 0.07
horse chestnut	22.1 ± 0.5	1.36±0.1	4.26 ± 0.1

Langmuir monolayer DPPC(d_{62})/CHOL(d_7) in NRW		
Subphase NRW (14% D)	layer thickness [Å]	*SLD* [10^{-6} Å^{-2}]
NRW	27.9 ± 2.0	3.77 ± 0.2
soapwort	30.9 ± 2.5	3.06 ± 0.2
soybean	27.3 ± 2.5	3.44 ± 0.2
oat	30.9 ± 2.0	3.10 ± 0.2
cowherb	29.1 ± 2.5	3.37 ± 0.2
horse chestnut	32.6 ± 2.0	3.08 ± 0.2
SLES	47.2 ± 4.0	1.19 ± 0.2

soybean extracts are 28 Å and 46 Å thick, respectively, pointing to a possible adsorption of larger molecules (see left column of Table 2).

The mechanical properties of the adsorbed layers were characterized by surface compression rheology. For this purpose, after 1 h adsorption at constant drop volume, the surface tension response to oscillatory changes of surface area was analyzed in a frequency range of 0.001 – 0.1 Hz and dry mass content $1\bullet10^{-3}$ - $3\bullet10^{\circ}$%. The resulting surface compression storage (*E'*) and loss (*E"*) moduli are shown in Fig. S3 and the values at the highest oscillation frequency (0.1 Hz) are collected in Fig. 2. For each extract at higher dry mass content values (> 0.1%), the storage modulus increases with frequency, clearly tending towards the high-frequency plateau (Gibbs elasticity, describing mechanical rigidity of the adsorbed layer). At the same time the loss modulus decreases tending towards 0, all in agreement with predictions of the Lucassen - van den Tempel theory [31]. This justifies approximating the Gibbs elasticity (E_0) with *E'* values for the highest oscillation frequency (0.1 Hz), collected in Fig. 2. Nevertheless, for some extracts (especially soybean, horse chestnut and cowherb) at lower dry mass content, *E"* slightly increases with increasing frequency. In these cases, the *E'*(0.1 Hz) likely underestimates E_0.

A clear inverse correlation between *E'* and the rate of Ostwald ripening in foams has been observed in the past for various mixed surfactant systems [32–35]. On this basis, Denkov et al. formulated a threshold criteria for mobile (E<50 mN/m) and rigid (E>100 mN/m) interfaces [1,33,36]. According to the adsorbed layer rigidity criteria mentioned above, the quinoa, cowherb, soapwort and soybean extracts above 0.1% d.m. content should form rigid adsorbed layers (Fig. 2). On the contrary, those of oat and horse chestnut should form mobile adsorbed layers in the whole range of dry mass tested (0.001–3%). In order to validate this hypothesis, we investigated foaming properties of the reconstituted extracts. The initial foam heights and their decay during 10 min are collected in Fig. 3. The initial foam heights for all extracts increase with increasing dry mass of the reconstituted extract, and for most extracts (except for oat and soapwort) the solutions are able to froth even at the lowest tested concentrations. The maximum foam heights are very similar for all extracts and the foams decay with rates inversely proportional to the dry mass content. With an exception of oat, practically no decay is observed on a 10 min timescale for the highest dry mass contents. Besides the horse chestnut extract (discussed more thoroughly in Supporting Materials), the foam stability agrees generally well with *E'* (0.1 Hz), in line with the threshold criterion described above. The only difference is that under our experimental conditions higher values of *E'* (exceeding 200 mN/m) are required to achieve the highest foam stability.

4.1. Model lipid monolayers

In the second part of the study, the effect of the reconstituted extracts on model lipid monolayers was analyzed. Because of the increasing use of saponin-rich extracts in cosmetic products applied directly to skin, we have selected for this purpose two model skin lipid mixtures [37,38]. The first model mimics the membrane lipids of keratinocytes present in deeper layers of epidermis and consists of a 7:3 (mol/mol) mixture of DPPC and cholesterol (DPPC/CHOL) [38]. The second model, consisting of ceramide AP, stearic acid and cholesterol, mixed in a molar ratio of 1:1:0.7 (CER/SA/CHOL), mimics the intercellular lipids "mortar" in the "bricks and mortar" model of the outermost layer of the epidermis [39]. The respective lipid mixtures spread on a Milli-Q subphase were first compressed to $\Pi_0 = 30$ mN/m, which is believed to induce packing of the lipid molecules similar to that in real biological bilayers [40]. The subphase was then continuously exchanged for the given reconstituted extract, reaching the final dry mass content of 1% while keeping the barriers in fixed position. The surface pressure values after 6000 s of the subphase exchange are collected in Fig. 4A, together with the corresponding values obtained under the same conditions in absence of the monolayers (Gibbs layers). The reference monolayers experiments with the subphase recirculation instead of exchange (i.e. exchanging subphase with pure Milli-Q water) show a slight reduction of surface

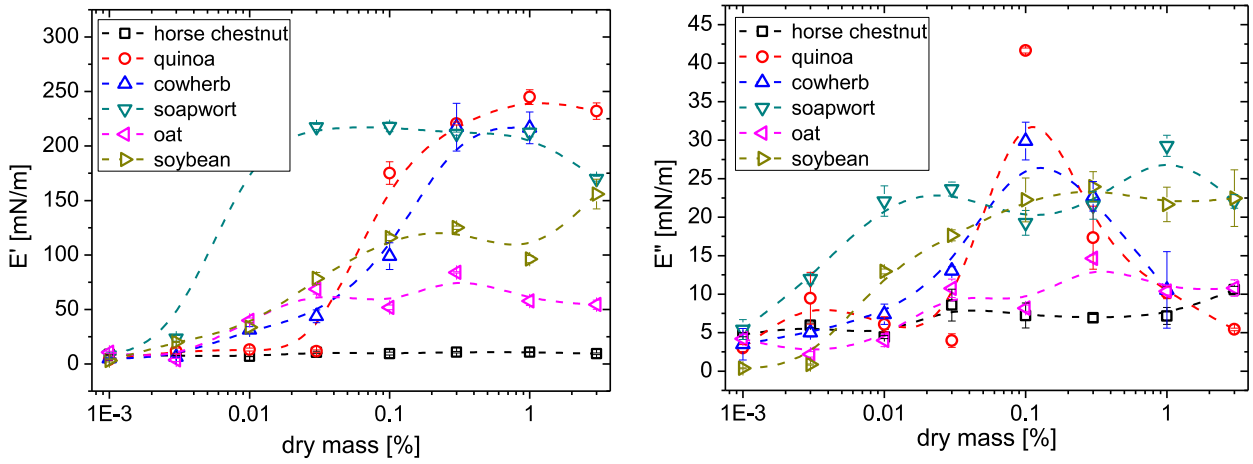

Fig. 2. The storage (*E'*) and loss (*E"*) compression moduli isotherms for the extracts employed in this study obtained at 0.1 Hz oscillation frequency.

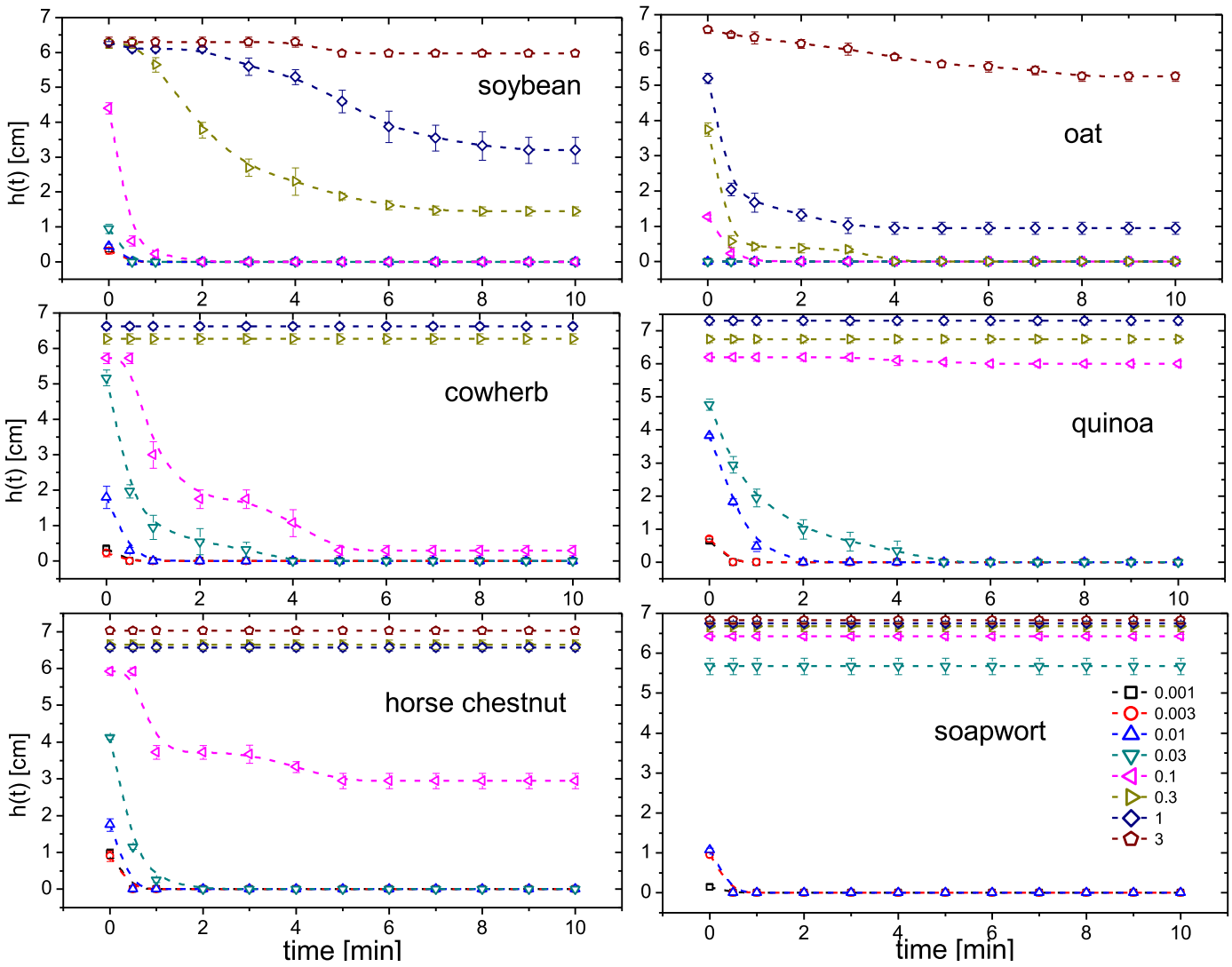

Fig. 3. Initial foam heights and their decay during 10 min for reconstituted extracts of soybean, oat, cowherb, horse chestnut, soapwort and quinoa at dry mass content in the range $1\bullet10^{-3}$ - $3\bullet10^{\circ}$%.

pressure below Π_0 during 6000 s (27 ± 2 and 25 ± 1 mN/m for DPPC/CHOL and CER/SA/CHOL, respectively), probably due to some relaxation processes within both monolayers. The surface pressure change is comparably low for the oat and, especially, soybean extracts, pointing to rather weak interactions of the components of these extracts with the lipid monolayers. On the other hand, very high surface pressure values are observed upon contacting both monolayers with the extracts of cowherb, soapwort or horse chestnut. In the latter case, the maximum surface pressure was even comparable to that observed previously for the highly purified Quillaja bark saponins (QBS) under similar conditions ($\Pi_0 = 32.5$ mN/m, DPPC/CHOL 4:1, $c_{QBS} = 0.2$%) [41]. Generally, the monolayers containing ceramide, stearic acid and DPPC responded with a more pronounced increase of surface pressure than those with DPPC and cholesterol. The strength of surface pressure response for different extracts is, however, not a simple reflection of surface activity (expressed as surface pressure) of the extract itself. For example, surface pressure for the Gibbs layers of the oat and soybean extracts in the absence of lipids is comparable to that of the horse chestnut, while the effect of the latter on the lipid monolayers is much higher than of the other two extracts (Fig. 4A). Generally, for all investigated extracts, the final surface pressure values were higher than for their corresponding Gibbs layers in absence of the lipid monolayer, suggesting that the lipids were not significantly solubilized by any extract.

The surface compression elasticity (E') of the monolayers after 6000 s exposure to the extracts provides additional information on mechanical properties of the penetrated monolayers. The results obtained at barrier oscillation frequency of 0.1 Hz collected in Fig. 4B show a limited alteration of compression surface elasticity for the soybean and oat extracts, and a significant increase for the remaining extracts, as compared with the corresponding monolayers on Milli-Q water. This corresponds well with the limited changes observed in surface pressure for oat and soybean, and confirms negligible interactions of their components with both lipid monolayers. The increase of E' values is especially pronounced for horse chestnut (CER/SA/CHOL monolayer) and for soapwort and cowherb (DPPC/CHOL monolayer). It is worth stressing that E' values for the penetrated monolayers exceed the sum of the values for the monolayers on water and for the Gibbs layers of the corresponding extract (in the absence of any lipids). This provides an additional evidence for the hypothesis of non-dissolution of the lipid monolayers by the tested extracts. Instead of being solubilized, the penetrated lipid monolayers are even mechanically strengthened by the extract components.

Additional details of the penetrated monolayers structure could be obtained from neutron reflectivity (NR) study, especially when using the deuterated lipids. To highlight the deuterated lipid monolayer, the neutron scattering length density (*SLD*) of the aqueous phase was

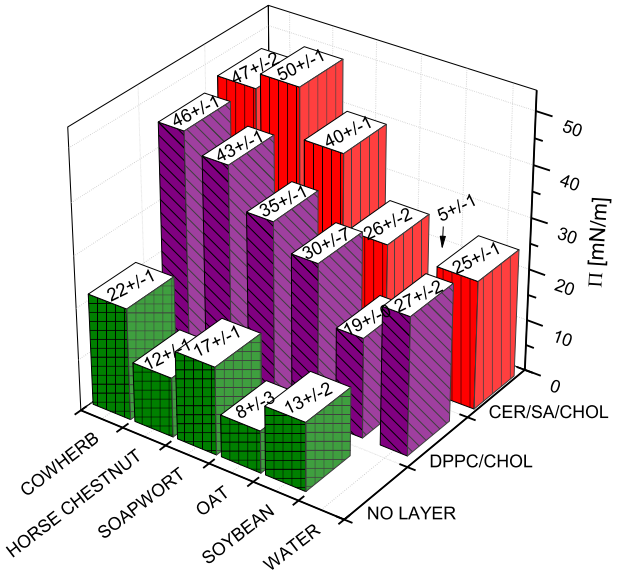

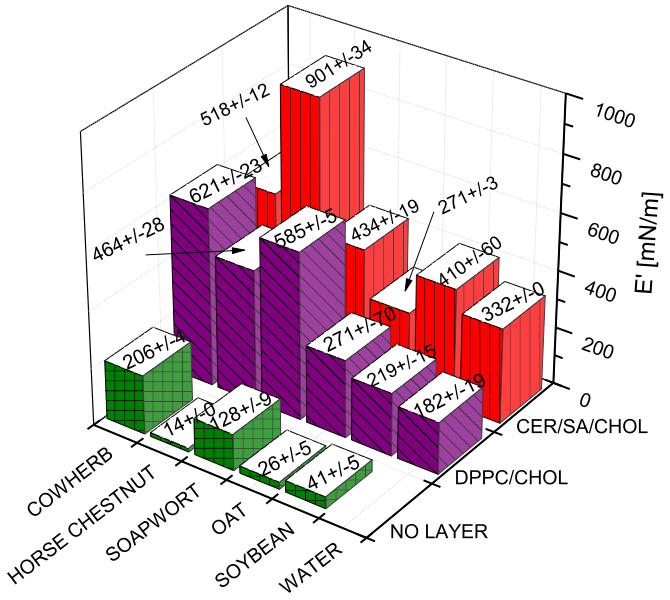

Fig. 4. Surface pressure (A) and compression storage modulus, E' (B) after 6000 s subphase exchange for Milli-Q water or 1% (w/w) plant extracts solutions in the absence of any lipid monolayer (Gibbs layers) and for DPPC/CHOL and CER/SA/CHOL monolayers compressed initially to $\Pi_0 = 30$ mN/m.

matched to that of air (null reflecting water, NRW) by using an appropriate D_2O/H_2O mixture. Such a combination of *SLD* enabled us to easily detect any changes within the monolayers structure (but not outside them). Fig. 5 compares the neutron *SLD* profiles for the DPPC-d_{62}/CHOL-d_7 (7:3) monolayers penetrated with the reconstituted extracts containing 1% d.m. (see Fig. S4 for the corresponding neutron reflectivity profiles and Table 2 for the best-fit parameters). For comparison, the analogous experiment was performed using a typical synthetic anionic surfactant, sodium laureth sulfate (SLES), currently employed in most body washing/shampoos formulations. The best-fit value of *SLD* for the bare monolayer ($3.77 \bullet 10^{-6}$ Å^{-2}) is only slightly lower than the theoretical value calculated from the isotopic composition of the lipid mixture ($3.96 \bullet 10^{-6}$ Å^{-2}), confirming that the lipids in the monolayer are not strongly hydrated. Upon penetration of the monolayer with the surface-active components of the extracts, *SLD* of the monolayer decreases in the order: soybean > oat ≈ cowherb ≈ horse chestnut > soapwort >> SLES. Interestingly, the monolayer thickness increases in the same order. The least pronounced changes can be observed again for the soybean extract. The slight reduction of *SLD* and practically no change of the layer thickness might seem at odds with the previously observed high thickness of the Gibbs layer formed at the bare soybean extract/air interface (without the lipid monolayer). One should, however, remember that the use of NRW renders the protium-containing material adsorbing from the soybean extract practically invisible beyond the monolayer ($SLD \approx SLD_{NRW} = 0$). Therefore, the present result does not exclude the presence of any protium-rich adsorbed layer extending beyond the lipid monolayer. It shows, however, that its presence within the lipid monolayer is only minor for soybean. Nevertheless, the different extent of *SLD* reduction and thickness increase observed for all extracts (Table 2) suggest that some protium-based (low-*SLD*) material, most likely originating from the extract components, enters the monolayer. The lower the *SLD* of the penetrated monolayer, the higher the content of the protium-based matter from the extract penetrating the deuterated lipid monolayer. Assuming that the lipid composition does not change upon penetration (i.e. that the DPPC/CHOL ratio remains the same), the amount of deuterated lipids within the monolayer should be proportional to the product of *SLD* and layer thickness. In that respect, the results for SLES clearly deviate from those for the extracts (the *SLD* × thickness product is only ~0.6 of the average value for the plant extracts), suggesting that SLES molecules did not penetrate but rather solubilized the deuterated lipids. This conclusion is in line with our previous observations of monolayer dissolution by SLES present in the subphase [3] and its known high detergent activity [42]. It should be stressed at this point that the layer thickness upon contact with any of the extracts is not reduced (Table 2), further confirming that the lipid monolayer is not removed by any of the investigated extracts.

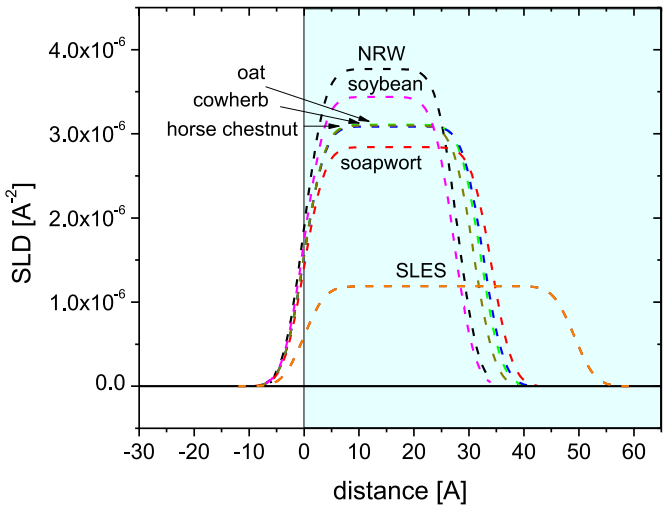

Fig. 5. Neutron scattering length density (*SLD*) profiles for the DPPC-d_{62}/CHOL-d_7 monolayers penetrated with the reconstituted extracts and SLES solution, all containing 1% dry mass in NRW.

4.2. Model lipid bilayers

The DPPC/CHOL monolayers used in the preceding chapter provide useful information on possible effects of the extracts on individual leaflets (half bilayers) of biological membranes of skin cells, e.g. keratinocytes. However, the tail-to-tail arrangement of the lipid monolayer pairs constituting real biological membranes may significantly alter their interaction with the extracts components. For this reason, in the third part of the study, we employed bilayers composed of DPPC and cholesterol (7:3 mol/mol) made from protiated (liposomes for dynamic light scattering) and deuterated (supported bilayers for neutron reflectivity) lipids.

The DLS analysis of the extract solutions (5% dry weight) shows that all tested plant extract solutions contain aggregates with sizes in the range 100–1500 nm (Fig. 6). The smallest aggregate size and polydispersity can be observed in the horse chestnut and soybean extracts, while oat and soapwort show the opposite characteristics (large size and broad size distribution). The particle size for the extruded DPPC/CHOL liposomes (D_{32}= 92 ± 14 nm, Fig. S5) is coherent with the pore size of the membrane used for extrusion (100 nm). The particle size distribution is clearly altered upon mixing the liposome dispersion with the extracts solutions. In most cases (except for horse chestnut) the particles detected in the mixtures display sizes intermediate between those of the bare liposomes and bare extracts (Fig. S5). The presence of single peaks with the size distribution narrowed in comparison to the bare extracts (Fig. 6) suggests that the aggregates found in the mixed systems might correspond to liposomes swollen by the extract components. This hypothesis is supported by the observations from Langmuir trough experiments (surface pressure and NR, see above), which proved that the corresponding monolayer can be penetrated by the extract components. Whether these aggregates take shapes similar to bicelles/nanodisks, as observed e.g. by the group of Hellweg for glycyrhizic acid or escin [43, 44], remains an open question and requires further investigations.

Based on previous experiments with lipid monolayers and liposomes, we have selected three extracts for the neutron reflectivity (NR) study of lipid bilayers at the Si/water interface (soapwort, horse chestnut and cowherb). The simultaneous fitting of the NR data for all three contrasts provided thickness of the head-group and tail-group region of, respectively, 10.5 and 19.5 Å, consistent with fully extended lipid molecules (see Fig. 7A and Supporting Materials for a more thorough description).

Having characterized the unexposed bilayers, we proceeded with studying their structural changes upon exposure to the selected reconstituted extract solutions. All surfactants were introduced at 0.3% and 1.0% dry mass contents (for soapwort additionally 0.1%). For all extracts, D_2O proved to be the most sensitive solvent to highlight changes in the NR profiles and the latter were affected already at 0.3% d.m., with little further changes at 1.0%. Analogously to the bare bilayers described above, the simultaneous fitting of the experimental data obtained for all neutron contrasts resulted in the scattering density profiles shown in Figs. S6–S14 Supporting Information (all best-fit parameters are collected in Table S2 and their summary is provided in Table S3, Supporting Information). Upon addition of saponin extract we observed a progressive increase of thickness of the tail-group region (up to 8%) at the expense of the head-group region (decrease of up to 16%, see Table S2 Supporting Information). Although this may be a meaningful difference, the change is quite subtle and any detailed discussion on the matter would be highly speculative. In interpreting the fitted parameters, one should take into account the fact that because of lack of neutron contrast, the *SLD* values for cholesterol and the triterpenoid region of saponins are very similar (Table S1), which makes them hardly distinguishable. Consequently, the adsorbed amounts of the three species (DPPC, cholesterol and saponin) within the bilayer cannot be determined independently. Nevertheless, because of the enhanced contrast between the d_{62}-DPPC and the other two components, at least the adsorbed phospholipid amount can be accurately determined. By monitoring the volume fraction of DPPC we can infer that the extract components (presumably saponins) either simply enter the bilayer or are exchanged for cholesterol, with only limited displacement of the phospholipid. Although we cannot directly judge which of the two mechanisms is operational, some indication can be inferred from the extent of hydration of the head-group region. Saponins, in contrast to cholesterol, possess a large hydrophilic glycosidic region which is expected to reside in the head-group region upon insertion into the bilayer (*SLD* varying between 1.54×10^{-6} Å^{-2} in H_2O and 3.00×10^{-6} Å^{-2} in D_2O). Replacement of cholesterol with saponins is thus expected to alter the *SLD* of the headgroup region with the extent dependent on the solvent used. With this information in hand we analyzed the NR data using two models, one assuming a fully symmetrical bilayer, which offers a smaller and more easily interpretable set of parameters, and the second - assuming asymmetry between the bilayer leaflet exposed to the solution of the saponin-rich extract. The latter model requires additional parameters but seems more realistic from a molecular perspective, as any surface-active components penetrating the bilayer are expected to accumulate preferentially in the solvent-facing leaflet. Fig. 7 presents the best-fit *SLD* profiles obtained using the asymmetrical model for the horse chestnut extract at both concentrations and soapwort at the

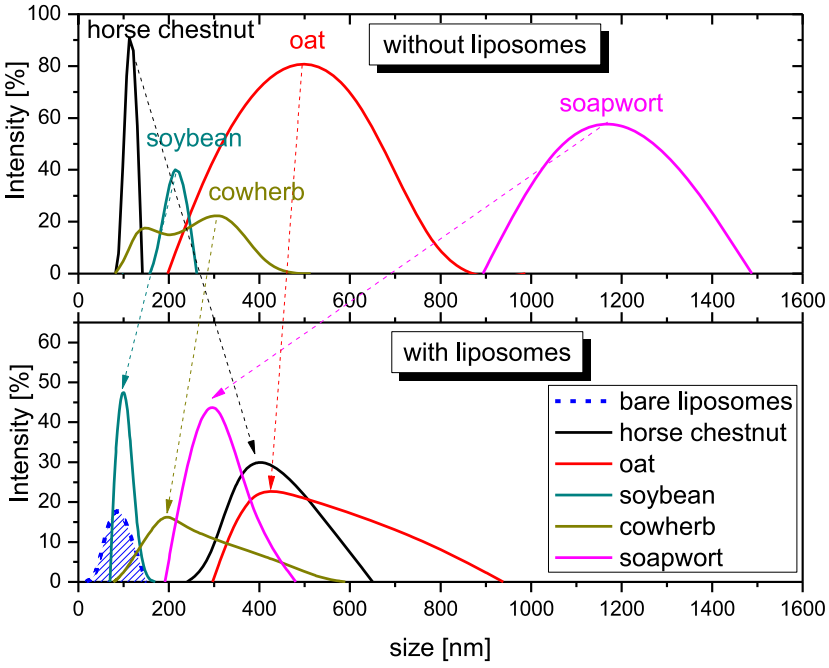

Fig. 6. (top) Particle size distribution in 5% (dry mass) solutions of extracts of cowherb, soapwort, horse chestnut, soybean and oat after 2 h of incubation at room temperature; (bottom) Particle size distribution in the same solutions 2 h after mixing with the DPPC/CHOL (7:3, mol/mol) liposomes (total lipid concentration $1 \circ 10^{-2}$%). All measurements performed in phosphate buffer (pH 7) at room temperature.

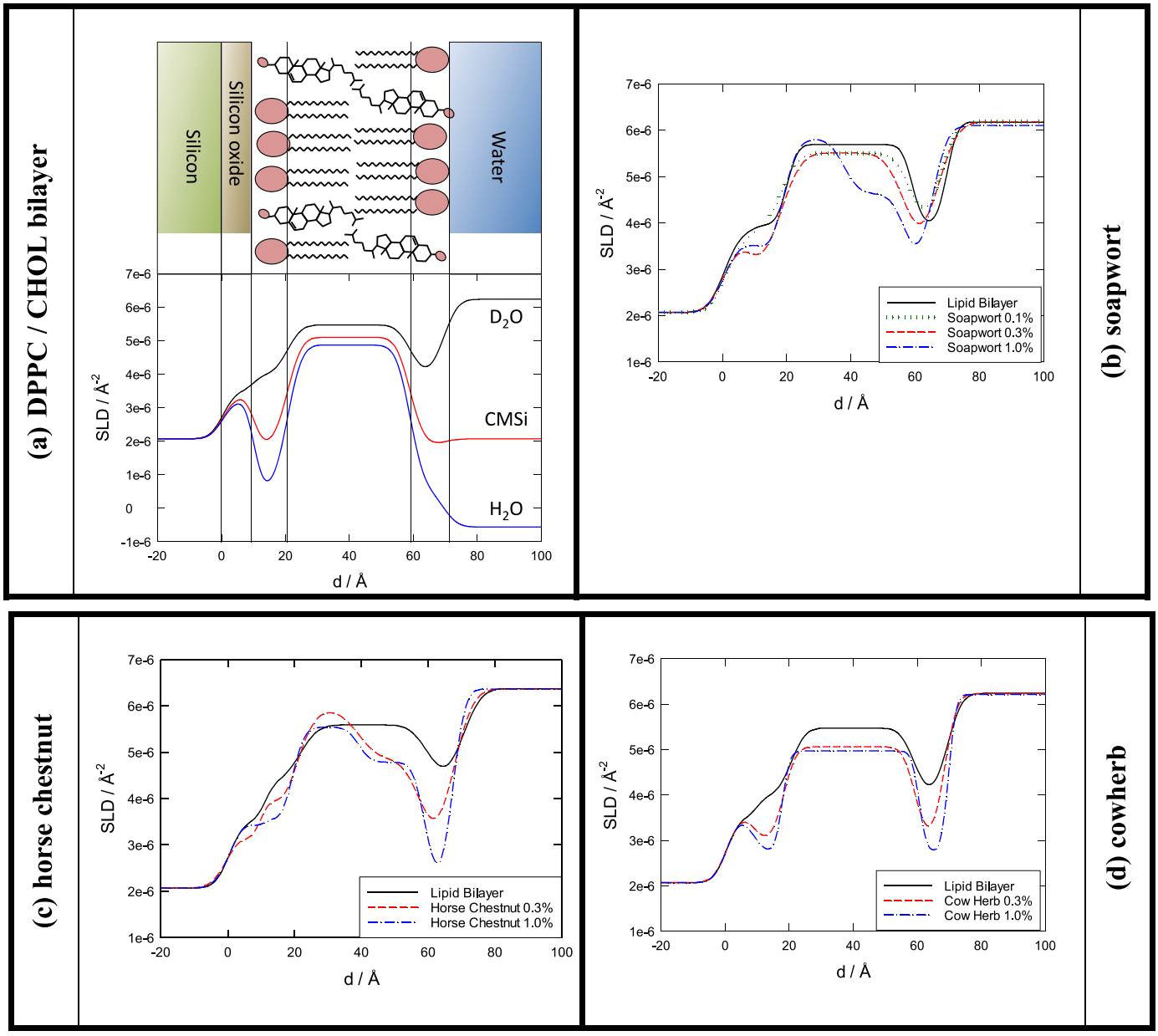

Fig. 7. *SLD* profiles for the bare DPPC/Chol bilayer in D_2O, CMSi and H_2O (a) and in soapwort (b), horse chestnut (c) and cowherb (d) extracts. Asymmetric profiles are shown for horse chestnut extract at both concentrations and soapwort at the highest concentration. In all other cases, where the introduction of asymmetry did not improve the fit quality, the symmetric profiles are shown.

highest concentration, and using the symmetrical model for all other extracts.

4.2.1. Symmetrical bilayer model

Upon injection of horse chestnut extract, the hydration in the lipid tail region is hardly affected, showing that the bilayer coverage does not change and it is stable against solubilization by the extract components. Given the impossibility to accurately determine the amount of cholesterol and saponin independently, we can use a significant reduction of the head group hydration (with all other structural parameters remaining constant within error) as an indication of changes in the headgroup region. The reduction may originate from insertion of saponins with their bulky glycosidic parts locating in the bilayer head-group region as the volume of the glycosidic region of a saponin molecule (approximated as a trisaccharide) is estimated to be twice as large as the DPPC headgroup. Even though the adsorbed amount of saponin within the bilayer cannot be reliably calculated from this data, it points towards an adsorption mechanism where saponins from horse chestnut are adsorbed onto the bilayer mostly via cholesterol substitution.

The bilayer coverage (as determined by the hydration in the tail group region) was also constant in the case of cowherb, again proving an overall stability of the bilayer. The volume fraction of DPPC in the tail-group was, however, found to decrease measurably, by about 10% and 13% at the dry mass content of 0.3% and 1.0%, respectively. The hydration of the head group region was also found to decrease with surfactant concentration, albeit to a lesser extent than observed for horse chestnut. These two observations seem to point out that a simple cholesterol/saponin substitution cannot explain the adsorption mechanism of the cowherb's components and some DPPC substitution probably also takes place.

Soapwort showed a similar behavior (~12% of lipid removal at the highest d.m. content) and the reduction in head group hydration was even more pronounced. With increasing extract concentration, water is clearly progressively expelled from the headgroup region. This leads to a

compaction of this layer due to replacement of small lipids headgroups (cholesterol's hydroxyl group and DDPC's phosphocholine) with a much bulkier saponins' glycosidic moiety. Although qualitatively the headgroup layer dehydration is comprehensible, the numerical values (between 0.02% and 1.90% for 1% d.m.) do not seem realistic for the intrinsically hydrophilic glycosidic moiety, questioning the validity of the symmetrical model. An additional argument against the model in the case of soapwort is a poor quality of the fit for the D_2O subphase in the q range between ~0.05 and ~0.14 $Å^{-1}$ (Fig. S7). The fit quality could not be improved, neither by introducing a hydration layer on silicon oxide, nor a surfactant-rich additional layer extending toward the aqueous phase (both invariably tended to disappear during fitting). Therefore, in the next step the model was extended to include bilayer asymmetry.

4.2.2. Asymmetrical bilayer model

The asymmetric model was applied to all samples at concentrations of 0.3% and 1.0%. The fit was only found to improve for soapwort at higher concentration and for both concentrations of horse chestnut, whereas practically no effect was observed for the other samples. Therefore, Fig. 7 shows the *SLD* profiles for the asymmetric model only for cases where this model fitted the experimental curves better than the symmetric one. For simplicity only the D_2O contrast is shown as it is the most sensitive to structural changes. The head-group and tail-group thickness differs little from the symmetric model, see Figs. S6–S8. For soapwort and horse chestnut the asymmetric model indicates preferential depletion of lipids from the outer leaflet, suggesting that the leaflet in direct contact with the extract is in fact enriched with its surface-active components. The situation is different for cowherb, where the fit was not improved by applying the asymmetric model and the lipid volume fraction was the same in the two leaflets within error. Apparently, the cowherb extract's components are rapidly distributed between the outer and inner leaflets. It is worth noting that the overall amount of lipid obtained from the asymmetric model, as averaged between the two leaflets, did not change with respect to the symmetrical bilayer. In all cases studied, the overall bilayer coverage is little affected with increasing the extract dry mass, confirming that the bilayers are indeed well tolerated by the extract components.

5. Discussion

All extracts for the present study were obtained using deionized water as the only extraction solvent. The spray-dried powders are thus free from any additives and contain only the plant components extractable with water. Our previous study investigated surface activity of analogous extracts obtained in presence of sodium benzoate and potassium sorbate employed as the preservative and drying aid [22]. However, because of the presence of these additional components, the effective extract concentration was lower than in the present set of extracts at the same dry mass content. It is thus not surprising that the UPLC-MS - determined saponin contents in the present extracts (Table 1) are systematically higher than those obtained in presence of preservatives [22]. The difference stems mainly from the fact that the preservatives constituted about half of the mass of the powdered extracts in the previous study, although the direct effect of sodium benzoate and potassium sorbate on extraction yield cannot be excluded. The surface tension and surface compression rheology results for 1% d.m. extract solutions are also in line with higher effective amounts of the surface active components as compared to the same extracts obtained in presence of preservatives [3] and [24] (see Supporting Materials for more detailed information).

Saponins are known for their exceptional ability to form highly surface-elastic adsorbed layers and the high E' values obtained in the present study for soapwort, quinoa and cowherb are in line with the literature values for purified triterpenoid saponins [30,36,45,46]. However, the low surface compression elasticity values for the horse chestnut even at the highest dry mass content are surprising, especially in combination with their relatively high total saponin content reported in Table 1. The present E' values (e.g. 10.8 ± 0.4 mN/m at 1% d.m.) are also lower than previously reported for the extracts obtained in the presence of sodium benzoate/potassium sorbate for the same dry mass (38.0 ± 3.2 [22]) and especially for the purified escin (> 150 mN/m [47]). On the other hand, the relatively high E' values for the oat and soybean extracts combined with their very low saponin contents suggest that they might contain some non-saponin surface active components capable of forming surface elastic adsorbed layers (e.g. proteins, which are also known to form layers with high E'). This hypothesis is supported also by the fact that their adsorption layers are thicker than for the other extracts in this study.

The surface pressure responses of the lipid monolayers observed for the presently employed extracts without preservatives/drying aids are generally more pronounced than these for the analogous extracts containing the additives, reported previously [22]. This is not surprising given the fact that the presence of sodium benzoate/potassium sorbate lowered effectively the extracted amount, and could also affect the extraction itself, as discussed above. However, the most important information from the surface pressure relaxation and surface compression rheology measurements of the penetrated lipid monolayers is that no lipid solubilization could be observed for any of the extracts. This confirms our previous observations for QBS [41], soapwort [3] and quinoa hulls [24] that the saponin-rich extracts generally do not solubilize the lipid monolayers, in contrast to some synthetic analogues [3,17]. Interestingly, the extracts with high saponin content were the most efficient in rising surface pressure and rigidifying the model lipid monolayers. In contrast, the soybean and oat extracts did not affect the model monolayers in any detectable way when probed by surface pressure, surface compression elasticity and neutron reflectivity.

Similar effects can be observed in bilayers, where the oat, soybean and cowherb extracts showed the least effect on size distribution of DPPC/cholesterol liposomes in DLS experiments. The latter, and especially the NR experiments, provided unequivocal proofs for the supported bilayer penetration for the soapwort, horse chestnut and cowherb extracts. In no case the presence of the extracts reduced the bilayer coverage: this clearly points toward expected good biocompatibility of the biosurfactants present in these extracts. Nevertheless, incorporation of the extracts components into the bilayer is accompanied by partial removal of lipids (~12–13% of DPPC for soapwort and cowherb and ~9% for horse chestnut). When the lipid bilayer interacts with soapwort and horse chestnut, the bilayer asymmetry gets more and more pronounced with increasing extract concentration, probably due to preferential accumulation of the extracts' components in the leaflet facing the aqueous solution. This process is accompanied by reduction of the headgroup hydration, which probably could be explained by a much higher volume of the glycosidic parts of saponins, as compared to the phosphocholine and cholesterol head-groups.

6. Conclusions

A careful optimization of the extraction and spray-drying conditions allowed us to obtain powdered extracts from six plants without any preservatives/drying aids. The reconstituted extracts were successfully characterized for their ability to lower surface tension and to form viscoelastic adsorbed layers. While all extracts except that of horse chestnut show similar surface tension isotherms (on the dry mass basis), the corresponding adsorbed layers differ significantly in their mechanical properties. The oat and soybean extracts are clearly much less abundant in saponins as compared to cowherb, horse chestnut, soapwort or quinoa, and show limited foaming abilities. They do not affect significantly the model lipid mono- and bilayers mimicking the skin outer layers, either. This lends support to the hypothesis suggesting that their surface activity is largely due to non-saponin biosurfactants of lower affinity to membrane lipids. In agreement with the known membrane activity of the horse chestnut extract, its effect on surface

compression modulus (*E'*) and surface pressure (Π) of both model membranes (DPPC/cholesterol, 7:3 mol/mol and Ceramide AP/stearic acid/cholesterol, 1:1:0.7 mol/mol/mol) is the most pronounced among the investigated extracts. At the same time, in bilayer studies this extract showed also the lowest lipid removal potential. The present results confirm that none of the tested extracts significantly solubilize the model lipid layers. Although further tests with more realistic skin models are necessary, the present data suggest that the extracts should not be harsh to the lipids of the human skin.

CRediT authorship contribution statement

Kamil Wojciechowski: Conceptualization, Methodology, Validation, Data curation, Writing – review & editing, Project administration, Funding acquisition. **Ilona Jurek:** Investigation, Methodology, Validation, Data curation, Writing – original draft. **Ilona Góral:** Investigation, Methodology, Validation, Data curation. **Mario Campana:** Investigation, Methodology, Validation, Data curation, Writing – original draft. **Thomas Geue:** Methodology, Software. **Thomas Gutberlet:** Data curation.

Declaration of Competing Interest

The Authors do not declare any conflict of interest

The authors declare that they have no known competing financial interests or personal relationships that could have appeared to influence the work reported in this paper.

Acknowledgments

This work was financially supported by The National Center for Research and Development (Poland), project "Development of a series of natural shampoos without the addition of synthetic surfactants, particularly SLS and SLES" (POIR.01.02.00–00–0005/16) and by Warsaw University of Technology. Prof. Anna Stochmal, Mrs Barbara Moniuszko-Szajwaj and Mr Bogdan Janda, are acknowledged for HPLC analysis. We wish to acknowledge the neutron beam time awarded by the ISIS Neutron Source (Experiments RB1910313, DOI 10.5286/ISIS.E.RB1920156). This work is based on experiments performed at the Swiss Spallation neutron source SINQ, Paul Scherrer Institute, Villigen PSI, Switzerland.

Supplementary materials

Supplementary material associated with this article can be found, in the online version, at doi:10.1016/j.surfin.2021.101486.

References

[1] N. Denkov, S. Tcholakova, D. Cholakova, Surface phase transitions in foams and emulsions, Curr. Opin. Colloid Interface Sci. 44 (2019) 32–47.
[2] X. Xu, Q. Sun, D.J. McClements, Enhancing the formation and stability of emulsions using mixed natural emulsifiers: hydrolyzed rice glutelin and quillaja saponin, Food Hydrocoll. 89 (2019) 396–405.
[3] I. Jurek, I. Góral, Z. Mierzyńska, B. Moniuszko-Szajwaj, K. Wojciechowski, Effect of synthetic surfactants and soapwort (Saponaria officinalis L) extract on skin-mimetic model lipid monolayers, Biochim. Biophys. Acta Biomembr. 1861 (2019) 556–564.
[4] Y. Ladjal Ettoumi, C. Berton-Carabin, M. Chibane, K. Schroën, Legume protein isolates for stable acidic emulsions prepared by premix membrane emulsification, Food Biophys. 12 (2017) 119–128.
[5] K. Klinchongkon, P. Khuwijitjaru, S. Adachi, B. Bindereif, H.P. Karbstein, U.S. van der Schaaf, Emulsifying properties of conjugates formed between whey protein isolate and subcritical-water hydrolyzed pectin, Food Hydrocoll. 91 (2019) 174–181.
[6] A. Audebert, A. Saint-Jalmes, S. Beaufils, V. Lechevalier, C.Le Floch-Fouéré, S. Cox, N. Leconte, S. Pezennec, Interfacial properties, film dynamics and bulk rheology: a multi-scale approach to dairy protein foams, J. Colloid Interface Sci. 542 (2019) 222–232.
[7] A. Szakiel, C. Pączkowski, M. Henry, Influence of environmental biotic factors on the content of saponins in plants, Phytochem. Rev. 10 (2011) 493–502.
[8] Ö. Güçlü-Üstündağ, G. Mazza, Saponins: properties, Applications and Processing, Crit. Rev. Food Sci. Nutr. 47 (2007) 231–258.
[9] B. Korchowiec, M. Gorczyca, K. Wojszko, M. Janikowska, M. Henry, E. Rogalska, Impact of two different saponins on the organization of model lipid membranes, Biochim. Biophys. Acta Biomembr. 1848 (2015) 1963–1973.
[10] C. De Groot, C.C. Müller-Goymann, Saponin interactions with model membrane systems - Langmuir monolayer studies, hemolysis and formation of ISCOMs, Planta Med. 82 (2016) 1496–1512.
[11] E.A.J. Keukens, T. De Vrije, L.A.M. Jansen, H. De Boer, M. Janssen, A.I.P.M. De Kroon, W.M.F. Jongen, B. De Kruijff, Glycoalkaloids selectively permeabilize cholesterol containing biomembranes, Biochim. Biophys. Acta Biomembr. 1279 (1996) 243–250.
[12] M. Orczyk, K. Wojciechowski, G. Brezesinski, Disordering effects of digitonin on phospholipid monolayers, Langmuir 33 (2017) 3871–3881.
[13] K. Wojciechowski, M. Orczyk, T. Gutberlet, G. Brezesinski, T. Geue, P. Fontaine, On the interaction between digitonin and cholesterol in langmuir monolayers, Langmuir 32 (2016) 9064–9073.
[14] J.M. Augustin, V. Kuzina, S.B. Andersen, S. Bak, Molecular activities, biosynthesis and evolution of triterpenoid saponins, Phytochemistry 72 (2011) 435–457.
[15] A.C.A. Yendo, F. de Costa, G. Gosmann, A.G. Fett-Neto, Production of plant bioactive triterpenoid saponins: elicitation strategies and target genes to improve yields, Mol. Biotechnol. 46 (2010) 94–104.
[16] A. Faizal, D. Geelen, Saponins and their role in biological processes in plants, Phytochem. Rev. 12 (2013) 877–893.
[17] K. Wojciechowski, M. Orczyk, T. Gutberlet, M. Trapp, K. Marcinkowski, T. Kobiela, T. Geue, Unusual penetration of phospholipid mono- and bilayers by Quillaja bark saponin biosurfactant, Biochim. Biophys. Acta Biomembr. 1838 (2014).
[18] W.S. Smith, D.A. Johnston, S.E. Holmes, H.J. Wensley, S.U. Flavell, D.J. Flavell, Augmentation of saporin-based immunotoxins for human leukaemia and lymphoma cells by triterpenoid saponins: the modifying effects of small molecule pharmacological agents, Toxins 11 (2019). Basel.
[19] S. Sama, G. Jerz, M. Thakur, M.F. Melzig, A. Weng, Structure-activity relationship of transfection-modulating saponins – a pursuit for the optimal gene trafficker, Planta Med. 85 (2019) 513–518.
[20] I. Góral, I. Jurek, K. Wojciechowski, How does the surface activity of soapwort (*Saponaria officinalis* L) extracts depend on the plant organ? J. Surfactant Deterg. 21 (2018) 797–807.
[21] I. Góral, K. Wojciechowski, Surface activity and foaming properties of saponin-rich plants extracts, Adv. Colloid Interface Sci. 279 (2020), 102145.
[22] I. Góral, A. Stochmal, K. Wojciechowski, Surface activity of the oat, horse chestnut, cowherb, soybean, quinoa and soapwort extracts – is it only due to saponins? Colloid Interface Sci. Commun. 42 (2021), 100400.
[23] M. Piotrowski, J. Lewandowska, K. Wojciechowski, Biosurfactant-protein mixtures: quillaja Bark Saponin at water/air and water/oil interfaces in presence of β-lactoglobulin, J. Phys. Chem. B 116 (2012).
[24] I. Jurek, I. Góral, K. Gęsiński, K. Wojciechowski, Effect of saponins from quinoa on a skin-mimetic lipid monolayer containing cholesterol, Steroids 147 (2019) 52–57.
[25] M. Gupta, T. Gutberlet, J. Stahn, P. Keller, D. Clemens, AMOR - The time-of-flight neutron reflectometer at SINQ/PSI, Pramana J. Phys. 63 (2004) 57–63.
[26] A.V. Makievski, V.B. Fainerman, R. Miller, M. Bree, L. Liggieri, F. Ravera, Determination of equilibrium surface tension values by extrapolation via long time approximations, Colloids Surf. A Physicochem. Eng. Asp. 122 (1997) 269–273.
[27] E.H. Lucassen-Reynders, A. Cagna, J. Lucassen, Gibbs elasticity, surface dilational modulus and diffusional relaxation in nonionic surfactant monolayers, Colloids Surf. A Physicochem. Eng. Asp. 186 (2001) 63–72.
[28] L.G. Parratt, Surface studies of solids by total reflection of X-rays, Phys. Rev. 95 (1954) 359–369.
[29] R. Stanimirova, K. Marinova, S. Tcholakova, N.D. Denkov, S. Stoyanov, E. Pelan, Surface rheology of saponin adsorption layers, Langmuir 27 (2011) 12486–12498.
[30] K. Wojciechowski, Surface activity of saponin from Quillaja bark at the air/water and oil/water interfaces, Colloids Surfaces B Biointerfaces 108 (2013) 95–102.
[31] M. van den Tempel, E.H. Lucassen-Reynders, Relaxation processes at fluid interfaces, Adv. Colloid Interface Sci. 18 (1983) 281–301.
[32] S. Tcholakova, Z. Mitrinova, K. Golemanov, N.D. Denkov, M. Vethamuthu, K. P. Ananthapadmanabhan, Control of Ostwald ripening by using surfactants with high surface modulus, Langmuir 27 (2011) 14807–14819.
[33] Z. Mitrinova, S. Tcholakova, K. Golemanov, N. Denkov, M. Vethamuthu, K. P. Ananthapadmanabhan, Surface and foam properties of SLES+CAPB+fatty acid mixtures: effect of pH for C12-C16 acids, Colloids Surf. A Physicochem. Eng. Asp. 438 (2013) 186–198.
[34] A. Stocco, D. Carriere, M. Cottat, D. Langevin, Interfacial behavior of catanionic surfactants, Langmuir 26 (2010) 10663–10669.
[35] D. Varade, D. Carriere, L.R. Arriaga, A.-.L. Fameau, E. Rio, D. Langevin, W. Drenckhan, On the origin of the stability of foams made from catanionic surfactant mixtures, Soft Matter 7 (2011) 6557–6570.
[36] N.D. Denkov, S. Tcholakova, K. Golemanov, K.P. Ananthpadmanabhan, A. Lips, The role of surfactant type and bubble surface mobility in foam rheology, Soft Matter 5 (2009) 3389–3408.
[37] J. Mueller, A. Schroeter, R. Steitz, M. Trapp, R.H.H. Neubert, Preparation of a new oligolamellar stratum corneum lipid model, Langmuir 32 (2016) 4673–4680.
[38] J. Sirieix-Plénet, J.C. Ader, C. Miquel, A. Mavon, N. Lauth-de Viguerie, Diffusion of E and Z urocanic amphiphiles through skin and their insertion in a membrane model, Skin Pharmacol. Physiol. 15 (2002) 425–433.
[39] G.M. El Maghraby, B.W. Barry, A.C. Williams, Liposomes and skin : from drug delivery to model membranes, Eur. J. Pharm. Sci. (2008) 203–222.

[40] D. Marsh, Lateral pressure in membranes, Biochim. Biophys. Acta Rev. Biomembr. 1286 (1996) 183–223.
[41] M. Orczyk, K. Wojciechowski, Comparison of the effect of two Quillaja bark saponin extracts on DPPC and DPPC/cholesterol Langmuir monolayers, Colloids Surf. B Biointerfaces 136 (2015) 291–299.
[42] F. Pan, Z. Li, H. Gong, J.T. Petkov, J.R. Lu, Membrane-lytic actions of sulphonated methyl ester surfactants and implications to bactericidal effect and cytotoxicity, J. Colloid Interface Sci. 531 (2018) 18–27.
[43] R. Sreij, C. Dargel, Y. Hannappel, J. Jestin, S. Prévost, R. Dattani, O. Wrede, T. Hellweg, Temperature dependent self-organization of DMPC membranes promoted by intermediate amounts of the saponin aescin, Biochim. Biophys. Acta Biomembr. 1861 (2019) 897–906.
[44] C. Dargel, Y. Hannappel, T. Hellweg, Heating-induced DMPC/glycyrrhizin bicelle-to-vesicle transition: a X-Ray contrast variation study, Biophys. J. 118 (2020) 2411–2425.
[45] K. Golemanov, S. Tcholakova, N. Denkov, E. Pelan, S.D. Stoyanov, Remarkably high surface visco-elasticity of adsorption layers of triterpenoid saponins, Soft Matter 9 (2013) 5738.
[46] K. Wojciechowski, M. Orczyk, T. Gutberlet, T. Geue, Complexation of phospholipids and cholesterol by triterpenic saponins in bulk and in monolayers, Biochim. Biophys. Acta Biomembr. 1858 (2016) 363–373.
[47] N. Pagureva, S. Tcholakova, K. Golemanov, N. Denkov, E. Pelan, S.D. Stoyanov, Surface properties of adsorption layers formed from triterpenoid and steroid saponins, Colloids Surf. A Physicochem. Eng. Asp. 491 (2016) 18–28.